SLAC-PUB-2144
June 1978
(T/E)

CONFIRMATION OF EXCHANGE DEGENERACY PREDICTIONS IN THE LINE-REVERSED REACTIONS: $\pi^+p \to K^+Y^*(1385)$ AND $K^-p \to \pi^-Y^*(1385)$ AT 11.5 GeV/c†

J. Ballam, J. Bouchez,[a] J. T. Carroll, C. V. Cautis, G. B. Chadwick, V. Chaloupka, R. C. Field, D. R. Freytag, R. A. Lewis,[b] M. N. Minard, K. C. Moffeit, and R. A. Stevens[a]

Stanford Linear Accelerator Center, Stanford University,

Stanford, California 94305

Abstract

We have measured in a single experimental setup the differential cross-sections and polarizations of the Y*(1385) produced in the two line-reversed reactions: $\pi^+p \to K^+Y^*(1385)$ (260 ev/μb) and $K^-p \to \pi^-Y^*(1385)$ (180 ev/μb) at 11.6 GeV/c. We compare these results to Σ^+ production in the same experiment. The data have been derived from a triggered bubble chamber experiment using the SLAC Hybrid Facility. We find that both helicity-flip and non-flip dominated processes are consistent with weak exchange degeneracy predictions.

(Submitted to Physical Review Letters)

† Work supported by the Department of Energy.

(a) Present address: DPhPE, CEN-Saclay, BP no. 2, F-91190, Gif-Sur-Yvette, France.

(b) Present address: Physics Department, Michigan State University, East Lansing, Michigan 48824.

As part of a systematic study of line-reversal in hypercharge exchange reactions, we present here results on Y*(1385) production in the reactions

$$\pi^+ p \to K^+ Y^*(1385) \quad (1)$$

$$K^- p \to \pi^- Y^*(1385) \quad (2)$$

at 11.6 GeV/c incoming momentum. In a Regge picture, the two reactions are expected to be dominated asymptotically by the exchange of the same two reggeons: the vector K*(890) and tensor K**(1420). Exchange Degeneracy (EXD) of these trajectories implies equal cross-sections for reactions (1) and (2) at the same value of the four-momentum transfer, t. The polarization of the final state hyperon should be either zero (strong EXD) or, if different from zero, it should have equal magnitude and opposite sign (weak EXD) in line-reversed reactions.[1] Our experiment was designed to test these relations.

Previous measurements of reactions (1) and (2) have mostly resulted from experiments done by different groups using different techniques,[2-4] thus making comparisons difficult to interpret. The present experiment is the first one to measure in a single detector the complete decay angular distribution of the Y*(1385) for both reactions (1) and (2), from which we determine the hyperon polarization. We also measure the differential cross-sections of the two reactions with a minimum of systematic differences between them. For comparison, we present differential cross-sections and hyperon polarizations from the reactions:

$$\pi^+ p \to K^+ \Sigma^+ \quad (3)$$

$$K^- p \to \pi^- \Sigma^+ \quad (4)$$

The Σ polarization results presented here include data additional to those in an earlier publication.[5] The experiment was conducted at the SLAC Hybrid Facility[6] consisting of the SLAC 1-m rapid cycling bubble chamber (15 Hertz),

triggered by data from electronic detectors processed on-line by a DGC-840 computer. The electronic fast trigger was given by an incoming π^+ (K^-) and a fast, forward K^+ (π^-), as defined by pulse height analyses of two Cerenkov counters. The triggering tracks were reconstructed on-line using thirteen planes of proportional wire chambers (PWC). The on-line algorithm triggered the bubble chamber camera lights after eliminating low momentum tracks, interactions outside the fiducial volume and non-interacting beam tracks. For the K^- run a μ-hodoscope behind 1m of iron has been used to reduce the triggering rate from K^- decays. The experimental setup is described in more detail elsewhere.[5,6]

The film was scanned for all events with a visible strange particle decay. These events were measured in three views on precision measuring tables and reconstructed by our geometry program. Tracks passing through the downstream system were constrained to fit the PWC data, giving a momentum resolution of $\sim$ 1.5% at 10 GeV/c. Events belonging to reactions (1) - (4) have been identified by kinematic fits, simultaneously at both primary and strange particle decay vertices. For reactions (1) and (2), the mass resolution of constrained events is $\sim$ 8 MeV in the Y*(1385) region.

The resulting sample is almost bias free and has well understood relative normalizations for all reactions. The data in both exposures have been corrected for: (a) fast trigger dead time, (b) PWC inefficiencies, (c) software trigger losses, (d) interaction or decay of the incident beam, (e) interaction or decay of the triggering particle, (f) random scanning and measurement losses, (g) strange particle decays too close or too far from the primary vertex. In addition, the K^- exposure was corrected for the hadron punch-through in the μ-hodoscope and the π^+ exposure for μ-contamination in the beam and for pion pile-up in the downstream Cerenkov counter. The overall

systematic uncertainty in our normalization is ± 10%.

The detector has ∿ 100% acceptance in the interval $0.01 < -t < 1$ GeV^2. We have corrected all distributions for the less of events with $-t < 0.01$ GeV^2 due to the triggering algorithm. In addition, we found small losses in the Λ sample which bias some of the angular distributions: asymmetric vees in which one of the tracks (mostly π^-) is too short to be properly measured or vees which do not open up sufficiently at the decay vertex and are misidentified as γ-conversions. These losses amount to $\lesssim$ 3% and have been taken into account when fitting angular distributions. The scanning loss in $\Sigma^+ \to p\pi^o$ has also been taken into account when measuring Σ^+ polarization.[5]

The present analysis is based on the sample of events described in Table I. We have made a model independent analysis of Y*(1385) production in reactions (1) and (2). The variables which we choose to describe the four-particle final state are: t- square of four-momentum transfer to the fast forward particle (K+ or π^-), $m_{\Lambda\pi^+}$- invariant mass of the $\Lambda\pi^+$ system and Ω - a set of four angles describing the cascade decay $Y^* \to \Lambda\pi^+$, $\Lambda \to p\pi^-$.[3]

We used the Extended Maximum Likelihood method[7] to separate Y*(1385) production as function of momentum transfer. All cuts imposed on the experimental sample were taken into account in the theoretical expressions. After each fit we have plotted the result of the fit on top of different experimental distributions and found good agreement with the data. The method of analysis, the variables used and the parametrization of the Y*(1385) are similar to those used by Holmgren et al.[3] The maximization of the log-likelihood function was done using the program OPTIME.[8]

The invariant mass distribution of the $\Lambda\pi^+$ system from both reactions (1) and (2) show a prominent peak due to Y*(1385) production, over a background level less than 10% of the signal (see Fig. 1). There is also some accumulation

of events at higher mass, primarily due to the Y*(1670) isobar. To obtain a good description of the mass spectrum up to 2 GeV, we tried several parametrizations for the background. We obtained the best fit with a p-wave Breit-Wigner[9] for the Y*(1385) and two simple Breit-Wigner functions in the $m_{\Lambda\pi} \sim 1.7$ GeV region, plus a constant phase-space term.

The results for the Y*(1385) did not depend on the parametrization used for the background. The parameters of the Y*(1385) and the high-mass enhancements were determined from fits in the region $m_{\Lambda\pi^+} < 2$ GeV and $-t < 1$ GeV^2. We find the mass and width of the Y*(1385) to be consistent within errors in the π^+ and K^- reactions. In the final fits we used the average values: $m_o = (1.380 \pm .002)$ GeV and $\Gamma = (.030 \pm .004)$ GeV.

With the mass and width of the Y*(1385) fixed, we have measured the differential cross-sections by fitting the amount of resonance production in several t-intervals up to $-t = 1$ GeV^2. The cross-sections for reactions (1) and (2) have been corrected for the Y*(1385) $\rightarrow \Lambda\pi$ and $\Lambda \rightarrow p\pi^-$ decay branching ratios (0.88 and 0.642, respectively). The results are shown in Figure 2a and 2b, together with the differential cross-sections from reactions (3) and (4). Only the decay $\Sigma^+ \rightarrow n\pi^+$ has been used in Figure 2a, to reduce systematic uncertainties.

The Σ^+ differential cross-sections show a simple exponential slope with some indication of flattening off for $-t > .4$ GeV^2. The Y*(1385) cross-sections show a forward dip, suggesting that the Y* vertex (as opposed to the Σ vertex) is helicity-flip dominated.

The Σ^+ differential cross-sections are nearly equal in slope and relative normalization while the Y*(1385) show significant differences at small $|t|$. Most of this difference is of kinematic origin: angular momentum conservation forces the two Y* cross sections to turn over at different values of momentum

transfer thus yielding different cross-sections at small $|t|$.

To describe this effect quantitatively, we did minimum χ^2 fits to the differential cross-sections using the function :

$$\frac{d\sigma}{dt} = \left(A_1 - A_2 \, (t - t_{min})\right) e^{bt} \qquad (5)$$

where A_1 and A_2 approximate the helicity non-flip and flip contributions, respectively. For the Y* reactions the slopes of the differential cross-sections were equal within errors, so that for the final fits we fixed them to the same value. The fits give a good description of the data as shown in Fig. 2b. In particular, the turnover at low t is well described by Equation (5), confirming thus the kinematic origin of the difference in cross-sections at low $|t|$ between reactions (1) and (2).

The values of A_1 and A_2 (see Table I) indicate that, within the limits of systematic uncertainties in this experiment, the data are in agreement with EXD predictions for both pairs of line-reversed reactions. (Note that the errors quoted in Table I are statistical only.)

To express quantitatively the difference between the K^- and π^+ induced reactions, we plot in Figures 2c and d the ratio:

$$< \cos \phi_{VT} > = \frac{d\sigma/dt(K^-) - d\sigma/dt(\pi^+)}{d\sigma/dt(K^-) + d\sigma/dt(\pi^+)} \qquad (6)$$

as function of -t. For small $|t|$ this quantity is a measure of the phase difference between the vector and tensor amplitudes[10] and EXD predicts $\phi_{VT} = \pi/2$. Apart from the rise at low $|t|$ in the Y* reactions, the data are consistent with this value. The solid line in Fig. 2d has been calculated from the fits shown in Fig. 2b.

Using A_1 as a representative value for the Σ cross-section and A_2 for the

Y*, we calculate: $\langle \cos \phi_{VT} \rangle = .05 \pm .10$ for reactions (1), (2) and $\langle \cos \phi_{VT} \rangle = -.02 \pm .10$ for reactions (3), (4). The quoted errors include the maximum systematic difference possible between the π^+ and K^- samples.

The only other experiment which has previously studied both pairs of reactions in a single experimental setup, is a missing mass experiment at 10.1 GeV/c.[4] They found in their experiment that reactions (1) and (2) violate EXD predictions while reactions (3), (4) are in approximate agreement. Our data show that most of the differences between both pairs of line-reversed reactions are of kinematic origin. Apart from kinematic differences, the cross-sections for both helicity flip (Y*) and non-flip (Σ) dominated processes are in good agreement with EXD predictions.

To measure the spin polarization of the final state hyperon, we have analyzed the decay angular distributions of the Σ^+ and of the cascade process $Y^*(1385) \rightarrow \Lambda\pi^+$, $\Lambda \rightarrow p\pi^-$. The Σ^+ analysis has been described elsewhere[5] and the result is shown in Figure 2e. For the Y*(1385) we have estimated density matrix elements (ρ_{mm}) by fitting the decay angular distribution of the Y* in the transversity frame.[11] We summarize our results in Figure 2f by plotting the Y* polarization defined as: $P = \frac{1}{J}\sum m \cdot \rho_{mm}$ where m is the spin-projection of the Y* along the normal to the production plane. The Σ^+ polarization is consistent with weak EXD predictions while the Y*(1385) has a polarization consistent with zero over the entire t-range for both reactions (1) and (2). This agrees with strong EXD: however, the Stodolsky-Sakurai[12] or Additive Quark Models[13] predict the same behavior.

In conclusion, our data for two pairs of line-reversed, hypercharge exchange reactions are consistent with exchange degeneracy predictions for both helicity-flip and non-flip amplitudes.

References

1. K.-W. Lai and J. Louie, Nuclear Physics B19, 205 (1970).

2. M. Aderholz et al., Nuclear Physics B11, 259 (1969),
   A. Bashian et al., Phys. Rev. D4, 2667 (1971),
   M. Aguilar-Benitez et al., Phys. Rev. D6, 29 (1972),
   D. Birnbaum et al., Phys. Letters 31B, 484 (1970),
   B. Chaurand et al., Nuclear Phys. B117, 1 (1976).

3. S. O. Holmgren et al., Nuclear Physics B119, 261 (1977).

4. A. Berglund et al., Phys. Letters 60B, 117 (1975), and
   A. Berglund et al., Phys. Letters 73B, 369 (1978).

5. P. A. Baker et al., Phys. Rev. Letters 40, 678 (1978).

6. G. B. Bowden et al., Nucl. Instr. and Methods 138, 75 (1976),
   J. Ballam and R. Watt, Annual Rev. Nucl. Scie. 27, 75 (1977),
   R. C. Field, SHF Memo 67, Internal Publication SLAC, Group BC, (1977).

7. J. Orear, Notes on Statistics for Physicists, UCRL-8417 (1958).

8. P. H. Eberhard and W. D. Koellner, Comp. Phys. Comm., 3, 296 (1972) and
   5, 163 (1973).

9. J. D. Jackson, Nuovo Cim., 34, 1644 (1964).

10. A. C. Irving and R. P. Worden, Physics Reports 34C, 117 (1977).

11. The normal to the production plane is defined as $n = B \times M$ where B is the beam direction and M is the direction of the particle recoiling against the Y* or Σ.

12. L. Stodolsky and J. J. Sakurai, Phys. Rev. Lett., 11, 90 (1963).

13. A. Bialas and K. Zalewski, Nucl. Phys. B6, 449 (1968).

TABLE CAPTION

Table 1. Statistics and Cross Sections. The integrated cross sections correspond to the interval $-t < 1$ GeV^2. Parameters A_1, A_2, b have been determined from fits according to Eq. (5) in the interval $-t < 0.4$ GeV^2 for the Σ reactions and $-t < 0.7$ GeV^2 for the Y*(1385) reactions.

TABLE I

Reaction	Events	Sensitivity (ev/μb)	Cross-Section* (μb)	A_1** ($\mu b/GeV^2$)	A_2** ($\mu b/GeV^4$)	b** (GeV^{-2})
$\pi^+ p \to K^+ \Sigma^+$ $\Sigma^+ \to p\pi^o$	1086	260.1	23.1 ± 1.9	246 ± 4	0	10.5 ± 0.3
$\pi^+ p \to K^+ \Sigma^+$ $\Sigma^+ \to n\pi^+$	1232					
$K^- p \to \pi^- \Sigma^+$ $\Sigma^+ \to p\pi^o$	715	180.2	27.0 ± 2.3	236 ± 8	0	9.8 ± 0.3
$K^- p \to \pi^- \Sigma^+$ $\Sigma^+ \to n\pi^+$	962					
$\pi^+ p \to K^+ Y^*(1385)$	936	260.1	7.0 ± 0.6	10 ± 1	326 ± 15	7.0 ± 0.4
$K^- p \to \pi^- Y^*(1385)$	911	180.2	10.1 ± 0.9	13 ± 3	362 ± 32	

*Error includes 10% systematic uncertainty.

**Statistical errors only.

FIGURE CAPTIONS

1. Invariant mass distribution of the $\Lambda\pi^+$ system. The solid line is the result of the maximum likelihood fit.

2. Comparison of differential cross sections and hyperon polarizations for the two pairs of line-reversed reactions (1) - (4).

   (a), (b). Differential cross sections. The Y* cross sections refer to the scale on the right. The lines are results of fits described in the text. The solid line is the fit to the π^+ data and the dashed one to the K^- data.

   (c), (d). Cross section asymmetry: $\langle \cos \phi_{VT} \rangle = \frac{d\sigma/dt(K^-) - d\sigma/dt(\pi^+)}{d\sigma/dt(K^-) + d\sigma/dt(\pi^+)}$. The solid line has been calculated using the results of fits to the differential cross sections.

   (e), (f). Hyperon polarization along the normal to the production plane.

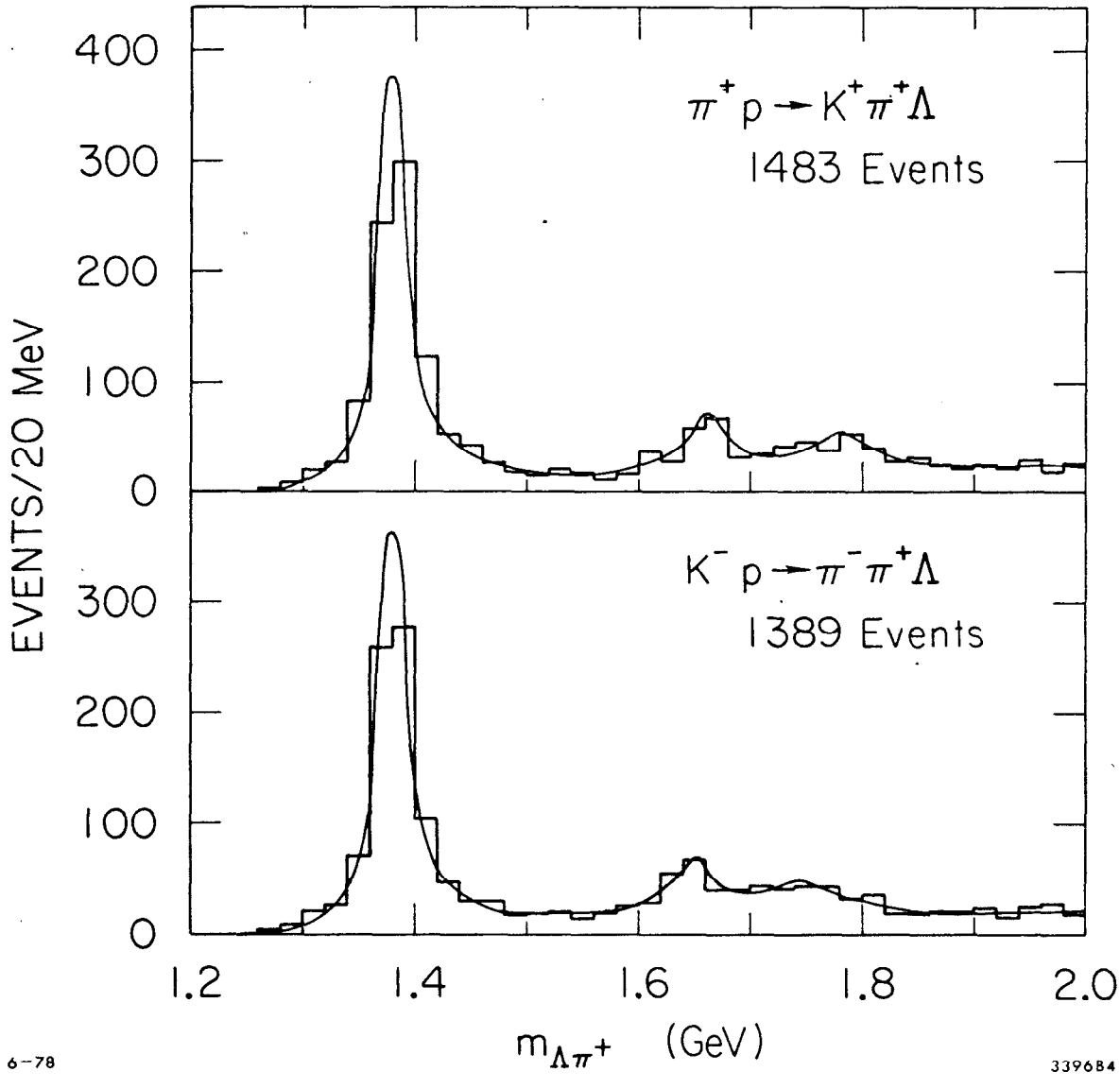
400
300
200
100
0
$\pi^+ p \rightarrow K^+ \pi^+ \Lambda$
1483 Events
300
200
100
0
$K^- p \rightarrow \pi^- \pi^+ \Lambda$
1389 Events
EVENTS/20 MeV
1.2
1.4
1.6
1.8
2.0
$m_{\Lambda\pi^+}$ (GeV)
6-78
339684

Fig. 1

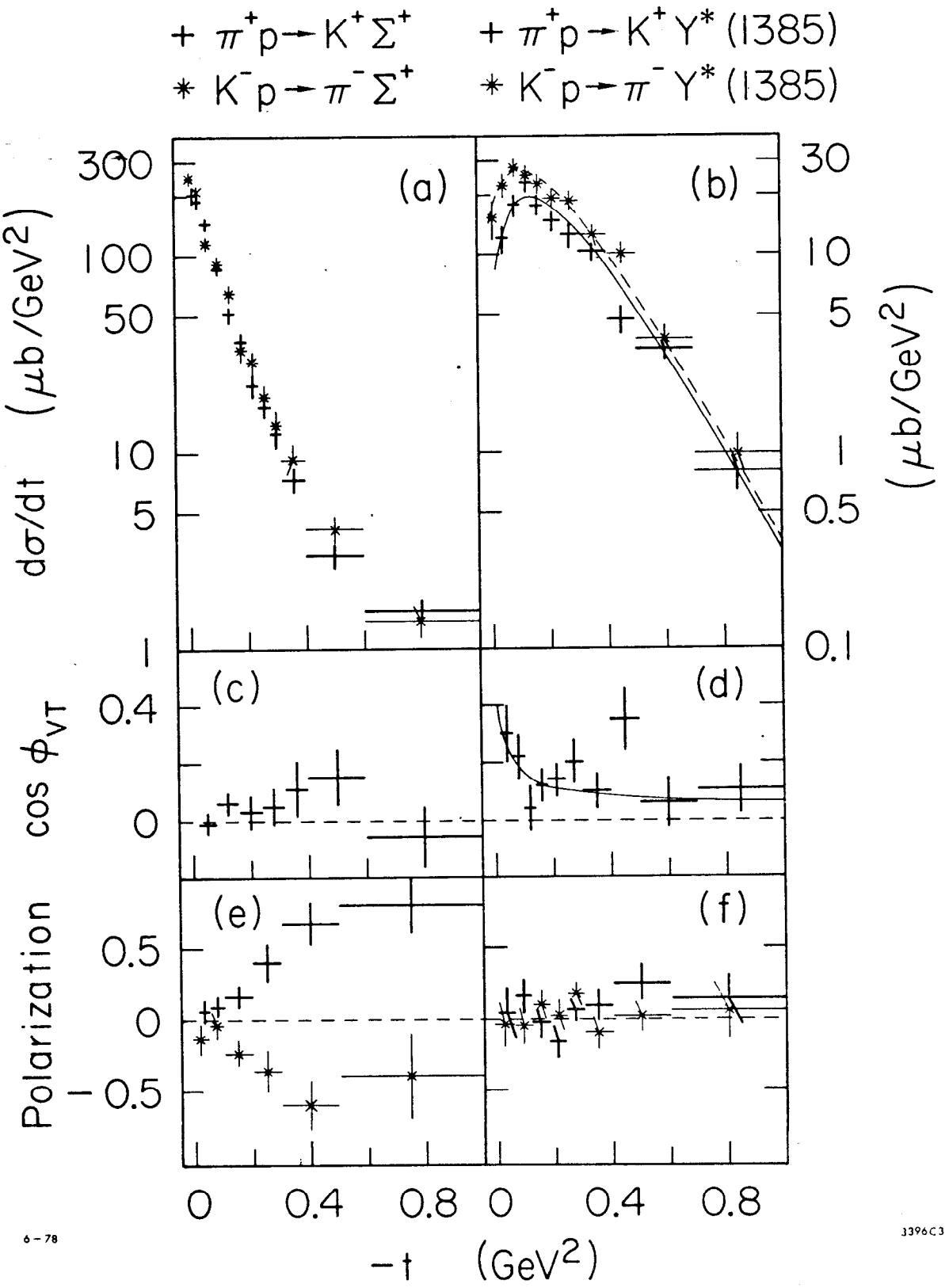
+ $\pi^+p \to K^+\Sigma^+$
+ $\pi^+p \to K^+Y^*(1385)$
* $K^-p \to \pi^-\Sigma^+$
* $K^-p \to \pi^-Y^*(1385)$
(a)
(b)
(c)
(d)
(e)
(f)
$d\sigma/dt$ ($\mu b/GeV^2$)
($\mu b/GeV^2$)
Polarization cos ϕ_{VT}
$-t$ (GeV^2)
300
100
50
10
5
1
30
10
5
1
0.5
0.1
0.4
0
0.5
0
−0.5
0
0.4
0.8
6-78
3396C3

Fig. 2